

Combined helium-atom-scattering and molecular-dynamics study of aluminum surface-phonon anharmonicities and linewidths

M. Gester

*Max-Planck-Institut für Strömungsforschung, Bunsenstrasse 10, W-37073 Göttingen, Germany
and University of Cambridge, Cavendish Laboratory, Madingley Road, Cambridge CB3 0HE, United Kingdom*

D. Kleinhesselink

*Max-Planck-Institut für Strömungsforschung, Bunsenstrasse 10, W-37073 Göttingen, Germany
and Department of Chemistry, University of California at Irvine, Irvine, California 92717*

P. Ruggerone and J. P. Toennies

*Max-Planck-Institut für Strömungsforschung, Bunsenstrasse 10, W-37073 Göttingen, Germany
(Received 10 December 1992; revised manuscript received 19 August 1993)*

The temperature dependence of the Rayleigh surface-phonon energies and widths have been measured with high-resolution helium-atom scattering for the $\bar{\Gamma}-\bar{X}$ direction and the $\bar{\Gamma}-\bar{M}$ directions on Al(100) and Al(111), respectively. Over a wide range of wave vectors the measured shifts and widths are in good agreement with a molecular-dynamics simulation based on a simple nearest-neighbor Morse potential. Contrary to previous reports of an enhanced shift in frequency with temperature on Cu(110), these results indicate that this measure of anharmonicity on close-packed aluminum surfaces is about 30% greater than that of the bulk.

In the bulk, anharmonicity affects many fundamental temperature-dependent phenomena, such as the coefficient of expansion, the specific heat, and the thermal conductivity. For the more loosely held atoms at the surface, anharmonicity is generally expected to be a factor 2 or more greater than in the bulk.¹ Recently there has been a great deal of interest in surface anharmonicity in connection with melting,² roughening³ and reconstruction phase transitions,⁴ surface magnetism,⁵ and multiphonon excitation in atom-surface collisions.⁶ So far there is only one electron-energy-loss-spectroscopy (EELS) experiment of surface-phonon frequencies and linewidths as a function of temperature, which is for the highly corrugated Cu(110) surface.⁷ However, for the clean low-index smooth metal surfaces there is only indirect evidence for anharmonicity coming from thermal-expansion measurements⁸ and observations of anomalous Debye-Waller attenuations of the scattered atom beams.⁹

In the present paper we report a helium-atom-scattering (HAS) study of the temperature-dependent anharmonic shifts in the frequency and the linewidth of surface Rayleigh phonons over a wide range of wave vectors on the (100) and (111) surfaces of aluminum. Aluminum was chosen for the following reasons: (1) As a nearly-free-electron metal, the surface phonons have recently become accessible to a first-principles calculation.¹⁰ Comparisons¹¹ of surface-phonon-dispersion curves with theory reveal that the (100) and (111) aluminum surfaces are nearly ideal terminations of the bulk with negligible relaxation¹² and surface-phonon softening.^{10,11} (2) The bulk phonons have been extensively studied with neutrons.^{13,14} (3) Clean aluminum surfaces are easily prepared and are very intense inelastic scatterers of He atoms.

The present experiments indicate anharmonic shifts of

the Rayleigh frequencies very similar to those reported in the recent EELS study of the highly corrugated Cu(110) surface.⁷ As a result of an incorrect evaluation¹⁵ of the bulk data, the authors of the EELS study reported that the temperature shift of phonon frequency is four to five times greater than in the bulk. A careful analysis of the data for Cu(110) reported in Ref. 15 provides a surface-to-bulk ratio of 2.21. This enhancement should be regarded as a large, though not anomalous, effect and could be due to the open and widely relaxed structure of the (110) surface. The data presented here and similar experiments on the Cu(100) surface¹⁵ indicate that, in fact, compared to the bulk the enhanced temperature shift resulting from anharmonicity for (100) and (111) metal surfaces is small. The observed anharmonicity is thus comparable to that in the bulk and about the same for the Cu(100) and the Al(100) and Al(111) surfaces.

The helium time-of-flight (TOF) scattering apparatus is essentially the same as the one described previously.¹⁶ The highly expanded helium nozzle beam has an energy spread of typically $\delta E = 0.8$ meV (full width at half maximum) at beam energies E_i of about 30 meV. The angle between incident and scattered beams was fixed at $\Theta_{SD} = 91.5^\circ$ and different parallel momentum transfers are accessed by simply rotating the crystal. The Al single-crystal samples (1 cm wide and 3 mm thick) were prepared in the same way as described previously.¹¹ The Auger spectra measured with a cylindrical mirror analyzer revealed C and O contaminations of less than 0.5%. The crystal temperature T_c was measured with a Ni/NiCr thermocouple and could be stabilized to within better than 2%. The surface structure was monitored *in situ* by LEED and He-atom diffraction.

Figure 1 shows two series of TOF spectra as a function of temperature for both surfaces. The well-resolved Ray-

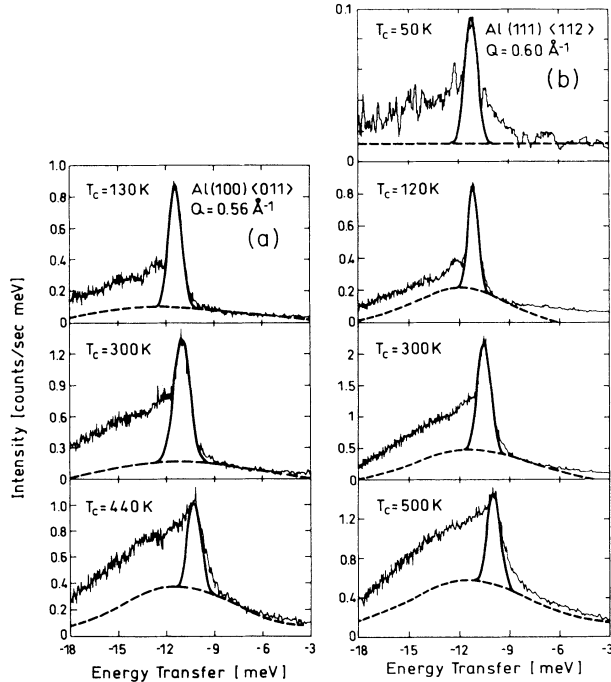


FIG. 1. Time-of-flight spectra transformed to an energy transfer scale obtained on (a) Al(100) $\langle 011 \rangle$ at three different crystal temperatures T_c , and (b) on Al(111) $\langle 112 \rangle$ at four different T_c in the figure. The incident beam energy was (a) 34.1 meV and (b) 26.9 meV, and the incident angles were about 39° corresponding to a nearly constant wave vector of the Rayleigh phonon of 0.56 and 0.60 \AA^{-1} , respectively. The heavy solid line shows a best fit of the Rayleigh wave peak and the multiphonon background is shown as heavy dashed line curves.

leigh phonon peak positions and widths were determined by fitting Gaussian distributions to the TOF spectra after these have been transformed to energy-transfer distributions. The results were corrected for the effect of the sloping bulk and multiphonon contribution to the left of and below the Rayleigh peak. This was estimated to lead to a small shift of at most 0.2 meV to large energies in the peak positions in the creation side of the spectra. The smooth background, indicated by the dashed line, is an estimate of the multiphonon background.⁶ The overall observed width δ_{exp} is composed of the natural phonon linewidth δ_{pho} and an additional width related to the resolution of the apparatus δ_{app} . With the assumption of independent Gaussian profiles, the natural phonon linewidth can be estimated from $\delta_{\text{pho}} = \sqrt{\delta_{\text{exp}}^2 - \delta_{\text{app}}^2}$, where δ_{app} was taken from measurements at the lowest temperature, e.g., 130 K for Al(100) and 50 and 120 K for Al(111), since they were in good agreement with calculations of the experimental resolution function.¹⁷

The experimental results of the Rayleigh phonon-dispersion curves, shown in Fig. 2 for three or four temperatures between 50 and 500 K for the two surfaces, are clearly separated from each other for $Q = 0.5 \text{ \AA}^{-1}$ out to the zone boundary. The spread in the points is less than 0.2 meV and an extrapolation to the zone boundary with the indicated best-fit curves provides for a precise

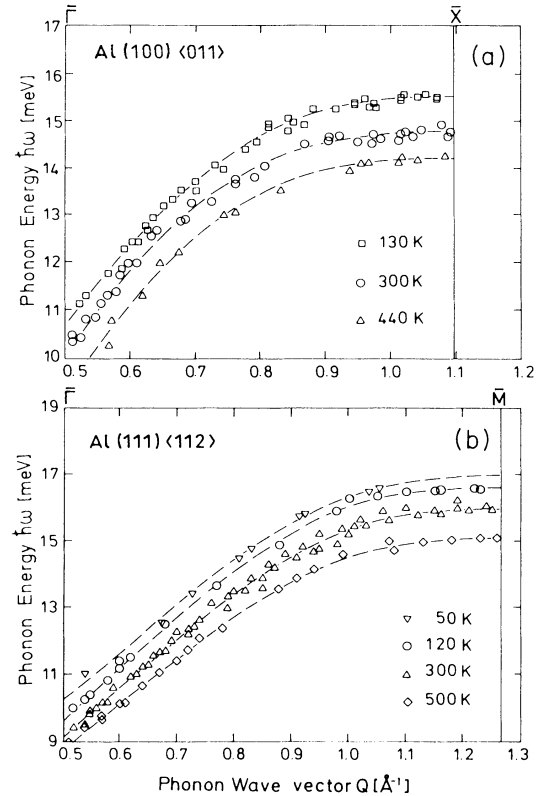


FIG. 2. Experimentally measured Rayleigh wave dispersion curves for several different temperatures for the (a) (100) Al surface and (b) (111) Al surface along $\bar{\Gamma}\text{-}\bar{X}$ ($\langle 001 \rangle$), and (b) for the (111) Al surface along $\bar{\Gamma}\text{-}\bar{M}$ ($\langle 112 \rangle$).

determination of the zone boundary frequencies. The temperature dependence of the zone boundary phonon energies determined in this way is shown by open circles on the right-hand side of Fig. 3. For the (100) surface the slope is $0.45 \pm 0.2 \text{ meV per } 100 \text{ K}$ at the \bar{X} point [Fig. 3(a)] and nearly the same for all wave vectors displayed in Fig. 2. $\bar{\Gamma}\text{-}\bar{X}$ is parallel to the bulk $\Gamma\text{-}K$ direction with the \bar{X} point corresponding to $\mathbf{q} = [\frac{1}{2}, \frac{1}{2}, 0]2\pi/a$. At this point the bulk anharmonicity of the T_2 mode is $0.34 \text{ meV per } 100 \text{ K}$ according to the data of Stedmann and Nilson.¹³ Thus the surface anharmonicity is about 30% larger than in the bulk. Extrapolation of the \bar{X} -point Rayleigh frequency to 0 K yields a value of $16.1 \pm 0.5 \text{ meV}$ in good agreement with the value of 16.3 meV predicted theoretically by Gaspar and Eguluz.¹⁸ At the \bar{M} point of the (111) surface the measured slope is the same as for the (100) surface, $0.45 \pm 0.2 \text{ meV per } 100 \text{ K}$. There are insufficient data for the equivalent bulk directions for comparison but it is not unreasonable to compare with the same $\Gamma\text{-}K$ direction as above. Extrapolation to 0 K yields a value of $17.2 \pm 0.4 \text{ meV}$ in reasonably good agreement with the theoretical values of 17.7 meV.¹⁸

The experimental linewidths are shown in Fig. 4. Only those points are shown for which the Rayleigh peak rose well above the multiphonon background so that the half-width was clearly apparent. Thus the data are restricted to small Q values at only two temperatures. Along the

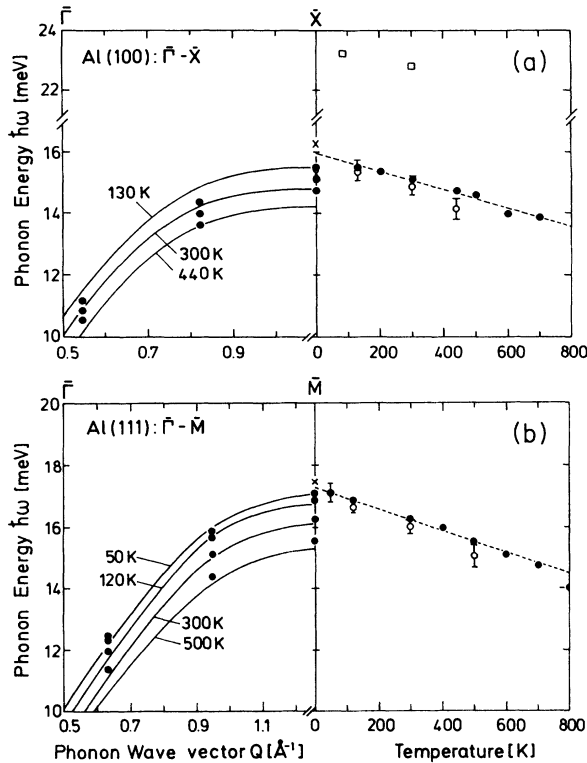


FIG. 3. Comparison of the MD-calculated phonon energies (solid circles) with the experimental Rayleigh dispersion curves (solid lines) for several different temperatures (a) for the (100) surface along $\bar{\Gamma}-\bar{X}$ ($\langle 011 \rangle$) and (b) for the (111) surface $\bar{\Gamma}-\bar{M}$ ($\langle 112 \rangle$). The solid curves in both figures are fits through experimental points and the individual points are calculated results. The right-hand part in each figure compares the zone boundary temperature dependences. The dashed lines are fits through the calculated points. The open symbols are the experimental results and the closed circles are the calculated points. The crosses at the zone boundary indicate the results of the density-response calculation of Gaspar and Eguluz (Ref. 18), and the squares in (a) show the neutron data for the bulk (Ref. 13).

$\bar{\Gamma}-\bar{X}$ direction of the (100) surface, a comparison with bulk measurements along the equivalent $\bar{\Gamma}-\bar{K}$ direction in the bulk is possible. For example, our averaged deconvoluted linewidths at $Q \approx 0.4 \text{ \AA}^{-1}$ are $0.46 \pm 0.10 \text{ meV}$ at 300 K and $0.98 \pm 0.13 \text{ meV}$ at 440 K. At a nearly corresponding bulk q value, Stedman and Nilsson¹³ found a difference of the linewidths at 80 and 300 K of $0.40 \pm 0.25 \text{ meV}$. Högborg and Sandström¹⁹ have predicted 0.72 meV, while an improved model of Koehler, Gillis, and Wallace²⁰ yields only 0.26 meV for the same difference. Thus, within the large uncertainties, the surface linewidths are comparable with those in the bulk.

Except for the Lennard-Jones model calculations of McGurn *et al.*²¹ and the recent embedded-atom calculations of Ditlevsen, Stoltze, and Nørskov²² and of Yang and co-workers,²³ we are not aware of any predictions of surface-phonon temperature-dependent anharmonicity effects on clean metal surfaces. For direct comparison with the present experimental results we have carried out a molecular-dynamics (MD) simulation, based on a

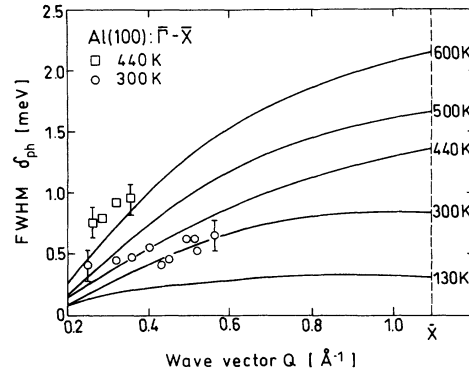


FIG. 4. Comparison of experimental (open symbols) and MD-simulated (solid lines) linewidths of the Rayleigh mode peaks as a function of wave vector for the (100) surface along the $\bar{\Gamma}-\bar{X}$ direction for two temperatures. The bars illustrate the errors estimated from the deconvolution of the apparatus resolution.

simple nearest-neighbor Morse potential function, $V(r) = D_e \{ \exp[-\beta(r - r_e)] - 1 \}^2$, to mimic the anharmonic interaction. A slab consisting of eight layers, each layer having $8 \times 8 = 64$ atoms, arranged in fcc(100) or fcc(111) geometries, was employed with periodic boundary conditions along the x and y directions with the z axis normal to the surface. The classical equations of motion were integrated using a time step of 10^{-15} sec. For the (100) surface, the force constant $k = 2\beta^2 D_e$ of the Morse function was chosen to yield the frequency for the Rayleigh wave at the \bar{X} point, extrapolated to 0 K. The well depth D_e was chosen to give the correct frequency at \bar{X} at a surface temperature of 300 K. Similarly, for the (111) surface, the force constant and well depth were chosen to give the correct values for the Rayleigh wave at \bar{M} at 0 and 500 K. The resulting potential parameters were $D_e = 2000 \text{ K}$ (0.172 eV) and $\beta = 1.80 \text{ \AA}^{-1}$ for the (100) surface, and $D_e = 2500 \text{ K}$ (0.215 eV) and $\beta = 1.69 \text{ \AA}^{-1}$ for the (111) surface. The bulk equilibrium internuclear separation $r_e = 2.859 \text{ \AA}$ was used for both potentials since relaxation is negligible for both surfaces.¹² The small differences in the potential parameters for the two surfaces are not surprising in view of the simplicity of the potential function.

The extraction of phonon parameters from the MD data is not a trivial task and the following scheme was employed.²⁴ First a harmonic lattice-dynamical slab calculation based on the same force constant of the corresponding Morse potential was used to determine the eigenvectors of the normal mode surface displacements. These eigenvectors are then used to project out the “normal” momenta for each desired mode from the Cartesian MD velocity components. Autocorrelation functions are computed every tenth time step from the normal momenta and subsequently Fourier transformed to yield the frequency and linewidth of each desired mode. The advantage in constructing these normal momenta and subsequently computing autocorrelation functions and Fourier transforms compared to the more traditional methods for analyzing MD data for phonons²³ lies in the fact that the resulting signal contains one well-defined frequency for

each desired normal mode, and not several frequencies.

The MD results for the Rayleigh phonon frequencies are indicated by the solid circles in Fig. 3. The overall agreement with the experimental data both for the dispersion curves [Fig. 3(a)] and the temperature dependence [Fig. 3(b)] is satisfactory. The temperature coefficients for the two modes obtained by a least-squares fit through the MD data are 0.30 meV/100 K for the mode at \bar{X} and 0.35 meV/100 K for the mode at \bar{M} , which is to be compared with the experimental result of 0.45 meV/100 K for both surfaces. We observe in our MD calculations that the strength of the temperature coefficient depends on the frequency of the phonon in the harmonic limit ($T \rightarrow 0$). For example, at \bar{M} , where the harmonic limit frequency is 17.27 meV, the temperature coefficient is somewhat greater than for the \bar{X} phonon with 15.97 meV. This trend holds for the Rayleigh wave phonons at other points along $\bar{\Gamma}$ - \bar{X} for the (100) surface and along $\bar{\Gamma}$ - \bar{M} for the (111) surface as well.

The experimental widths for the (100) surface are compared with the theoretical results in Fig. 4. Because of the falloff in phonon intensity with Q the measurements were limited to $Q \leq 0.56 \text{ \AA}^{-1}$. At 300 K the agreement with theory is surprisingly good. The MD simulations predict a linear increase in the width with temperature at low temperatures and an increase faster than linear at higher temperatures for the (100) surface. A linear fit through the calculated widths for the four lowest temperatures gives 0.38 meV/100 K for the temperature coefficient of the (100) surface at \bar{X} . The few results at 440 K shown in Fig. 4 suggest that the experimental temperature dependence is greater than predicted. The experimental and theoretical results for the (111) surface are very similar to those shown in Fig. 4.

The success of the Morse potential MD simulations is

at first surprising, since to fit Al phonon-dispersion curves long-range interactions involving up to ten nearest neighbors are known to be required.¹¹ The good agreement with the MD calculations indicates that anharmonicity can be successfully described by only a single effective anharmonicity parameter, which, for a Morse potential, is conveniently given by $x_e = \hbar\beta^2/2\mu\omega_0$, where ω_0 is the harmonic frequency and μ is a reduced effective mass.

In conclusion, we have shown that the smooth aluminum surfaces, contrary to general expectations,¹ exhibit a temperature-dependent shift and width in the Rayleigh phonon frequency, which is only slightly larger than in the bulk. The comparison with the recent EELS results on Cu(110) (Ref. 7) shows that in fact the temperature line shifts are nearly identical, e.g., 0.50 meV per 100 K for Cu(110) compared to about 0.45 meV per 100 K for both Al(100) and Al(111). Phonon linewidths of 0.20–0.6 meV have been measured as a function of phonon wave vector up to $Q = 0.56 \text{ \AA}^{-1}$ for Al(100) in good agreement with the theory. Extrapolation to the zone boundary indicates a linewidth of about 0.8 meV at 300 K. Thus it appears as if the intrinsic EELS phonon linewidths for Cu(110) of 6.5 meV (300 K) at the \bar{Y} point may be in error as also suggested in Ref. 23. The present experiments and theory are also in excellent agreement with recent MD calculations²³ using a different method than described here.

We thank D. Himes for calculating the multiphonon background in Fig. 1, G. Benedek for numerous enlightening discussions, A. Franchini for information about the comparison with the bulk data, and A. Lock for help with the experiments. P.R. thanks the Alexander von Humboldt Stiftung for financial support.

¹R. E. Allen and F. W. de Wette, *Phys. Rev.* **188**, 1320 (1969).
²C. S. Jayanthi, E. Tosatti, and L. Pietronero, *Phys. Rev. B* **31**, 3456 (1985).
³G. Armand, D. Gorse, J. Lapujoulade, and J. R. Manson, *Europhys. Lett.* **3**, 1113 (1987).
⁴A. Fasolino and E. Tosatti, *Phys. Rev. B* **35**, 4264 (1987).
⁵G. Benedek, J. P. Toennies, and G. Zhang, *Phys. Rev. Lett.* **68**, 2644 (1992).
⁶V. Celli, D. Himes, P. Tran, J. P. Toennies, Ch. Wöll, and G. Zhang, *Phys. Rev. Lett.* **66**, 3160 (1991).
⁷A. P. Baddorf and E. W. Plummer, *Phys. Rev. Lett.* **66**, 2770 (1991).
⁸Y. Cao and E. Conrad, *Phys. Rev. Lett.* **65**, 2808 (1990).
⁹G. Armand and J. R. Manson, *Phys. Rev. Lett.* **53**, 1112 (1984); D. Gorse and J. Lapujoulade, *Surf. Sci.* **162**, 847 (1985).
¹⁰J. A. Gaspar, A. G. Eguluz, M. Gester, A. Lock, and J. P. Toennies, *Phys. Rev. Lett.* **66**, 337 (1991).
¹¹A. Lock, J. P. Toennies, Ch. Wöll, V. B. Bortolani, A. Franchini, and G. Santoro, *Phys. Rev. B* **37**, 7087 (1988).
¹²(111): H. B. Nielsen and D. L. Adams, *J. Phys. C* **15**, 615 (1984); (100): A. Bianconi and R. Z. Bachrach, *Phys. Rev. Lett.* **42**, 104 (1979).
¹³R. Stedman and G. Nilsson, *Phys. Rev.* **145**, 492 (1966).

¹⁴K.-E. Larsson, U. Dahlborg, and S. Holmryd, *Ark. Fys.* **17**, 369 (1960).
¹⁵G. Benedek and J. P. Toennies, *Phys. Rev. B* **46**, 13 643 (1992).
¹⁶J. P. Toennies, in *Surface Phonons*, edited by W. Kress and F. W. de Wette, Springer Series in Surface Sciences Vol. 21 (Springer, Berlin, 1991).
¹⁷D. M. Smilgies and J. P. Toennies, *Rev. Sci. Instrum.* **59**, 2185 (1988).
¹⁸J. A. Gaspar and A. G. Eguluz, *Phys. Rev. B* **40**, 11 976 (1989).
¹⁹T. Högborg and R. Sandström, *Phys. Status Solidi* **33**, 169 (1969).
²⁰T. Koehler, N. S. Gillis, and D. C. Wallace, *Phys. Rev. B* **1**, 4521 (1970).
²¹A. R. McGurn, A. A. Maradudin, R. F. Wallis, and A. J. C. Ladd, *Phys. Rev. B* **37**, 3964 (1988).
²²P. D. Ditlevsen, P. Stoltze, and J. K. Nørskov, *Phys. Rev. B* **44**, 13 002 (1991).
²³L. Yang and T. S. Rahman, *Phys. Rev. Lett.* **67**, 2327 (1991); L. Yang, T. S. Rahman, and M. S. Daw, *Phys. Rev. B* **44**, 13 725 (1991).
²⁴D. Kleinhesselink, P. Ruggerone, and J. P. Toennies (unpublished).